

The Hunt for Red October II: A magnetohydrodynamic boat demonstration for introductory physics

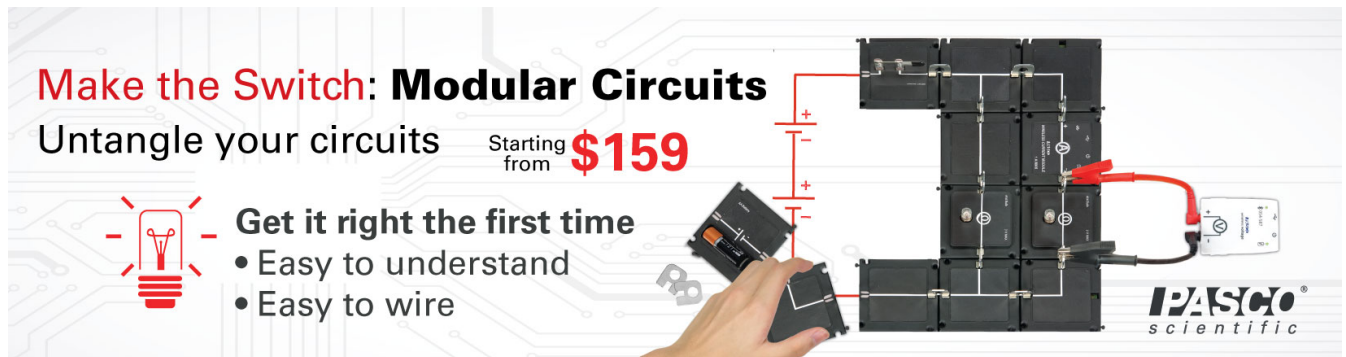
James Overduin, Viktor Polyak, Anjalee Rutah, Thomas Sebastian, Jim Selway, and Daniel Zile

Citation: *The Physics Teacher* **55**, 460 (2017); doi: 10.1119/1.5008337

View online: <http://dx.doi.org/10.1119/1.5008337>

View Table of Contents: <http://aapt.scitation.org/toc/pte/55/8>

Published by the [American Association of Physics Teachers](#)



Make the Switch: Modular Circuits

Untangle your circuits

Starting from **\$159**

Get it right the first time

- Easy to understand
- Easy to wire

PASCO
scientific

The Hunt for Red October II: A magnetohydrodynamic boat demonstration for introductory physics

James Overduin, Viktor Polyak, Anjalee Rutah, Thomas Sebastian, Jim Selway, and Daniel Zile, Department of Physics, Astronomy and Geosciences, Towson University, Towson, MD

The 1990 film “The Hunt for Red October” (based on Tom Clancy’s 1984 debut novel of the same name) featured actors like Sean Connery and Alec Baldwin, but the star of the movie for physicists was a revolutionary new magnetohydrodynamic (MHD) marine propulsion system. The so-called “caterpillar drive” worked with no moving parts, allowing a nuclear missile-armed Soviet submarine to approach the U.S. coast undetected. As the submarine captain (played by Connery) said, “Once the world trembled at the sound of our rockets ... now they will tremble again—at the sound of our silence.”¹

MHD propulsion is not fictional: real-life prototypes include the *EMS-1*, a 3.0-m submarine that achieved speeds of 0.4 m/s during tests in California in 1966,² and the *ST-500*, a 3.6-m boat that reached 0.6 m/s in Japan in 1979.³ The world’s first and so far only full-sized MHD-propelled craft, *Yamato-1*, carried 10 people at speeds of up to 15 km/h during successful sea trials in Kobe, Japan, in 1992.⁴

The *Yamato-1* has since been put up on blocks (Fig. 1) and interest in this form of marine propulsion has apparently waned. Why? Motivated by this question, and by the possibility of engaging students with a simple but dramatic demonstration, we built and tested a small-scale MHD boat that can easily be replicated by instructors at low cost in a classroom setting. Our treatment differs in emphasis and is complementary to an excellent earlier article in this journal by Font and Dudley.⁵ Other useful discussions are in Refs. 6–10 and a typical textbook account appears in Ref. 11.

Theory

As with a rocket, the principle underlying MHD propulsion is Newton’s third law: propellant is forced backward out of the thruster, exerting an equal and opposite force forward on the boat. In this case, the propellant is provided by Na^+ and Cl^- ions present in seawater. After entering the thruster, these ions (with charge $q = \pm e$) are accelerated sideways



Fig. 1. The MHD-propelled *Yamato-1* on display in Kobe, Japan.

by an electric field, and then (once their velocities \mathbf{v} have a transverse component) backward out of the thruster by an orthogonal magnetic field \mathbf{B} according to the Lorentz force law $\mathbf{F}_m = q\mathbf{v} \times \mathbf{B}$ (Fig. 2).

Ion velocity \mathbf{v} relative to the boat can be resolved into components v_{\parallel} (anti-parallel to the motion) and v_{\perp} (transverse). Then the Lorentz force has components $F_{\perp} = eBv_{\parallel}$ and $F_{\parallel} = eBv_{\perp}$ (Fig. 3). The transverse components F_{\perp} acting on the Na^+ and Cl^- ions are opposite and almost equal, so they produce little net thrust on the boat. The longitudinal components F_{\parallel} , however, point the same way and provide the thrust. If the total number of ions affected is N , then their transverse motion creates a current $I = Nev_{\perp}/L$, where L is the distance between electrodes. The thrust may then be expressed as

$$F_{\parallel} = F_m \sin \theta = NeBv_d = ILB, \quad (1)$$

where we have identified v_{\perp} with the drift velocity v_d of the ions. While this can be regarded as constant on average, the motions of individual ions are anything but uniform. To begin with, they are surrounded by “hydration shells” of strongly bound H_2O molecules that move along with them.¹² Secondly, they are buffeted by random collisions with water molecules that are much more energetic than their motions due to the applied electric field (since $\frac{3}{2}k_B T \gg \frac{1}{2}mv^2$ at liquid water temperatures). Thirdly, they also interact with each other. On average, though, these effects combine to produce a frictional retarding force that can be described by Stokes’ law $F_s = 6\pi\eta r v$, where η is viscosity and r a characteristic radius.¹³ This

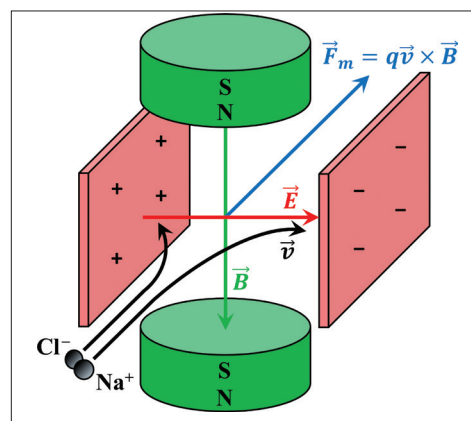


Fig. 2. Schematic depiction of the direct-current duct-type MHD drive. Incoming ions (bottom left) are pushed sideways by the electric field and then backward out of the thruster by the magnetic field (right-hand rule).

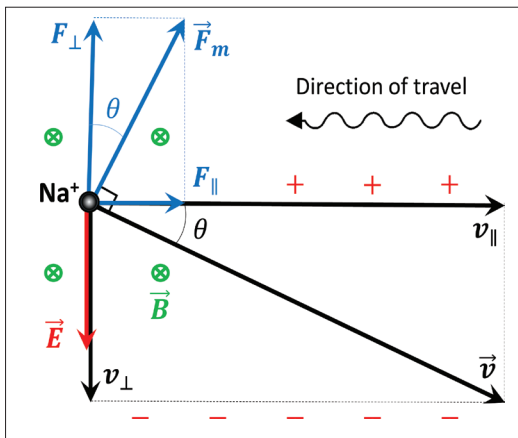


Fig. 3. Key vectors and their components. In the boat frame, the sodium ion moves longitudinally at a speed v_{\parallel} and in a transverse direction at v_{\perp} (under the influence of E). The magnetic field B then acts on the ion with a Lorentz force F_m whose components are $F_{\perp} = eBv_{\parallel}$ and $F_{\parallel} = eBv_{\perp}$.

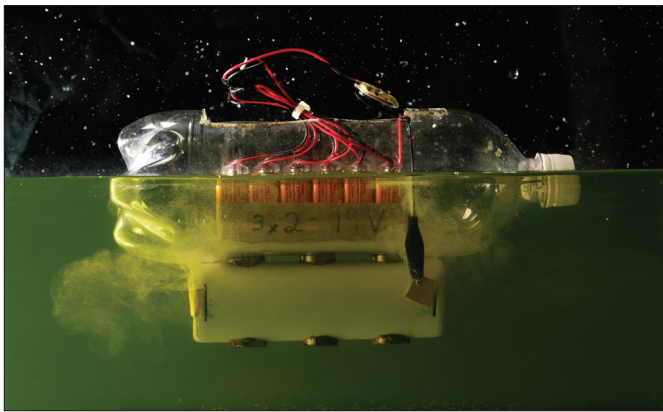


Fig. 4. MHD boat in action, traveling from left to right. Note bubbles escaping from the rear of the thruster tube at left.

retarding force rapidly comes into equilibrium with the applied force $F_e = eE$. Setting $F_s = F_e$ gives the drift velocity as $v_d = eE/6\pi\eta r$.

We will have more to say about drift velocity below, but for now we note that thrust F_{\parallel} is most conveniently expressed in terms of the current I , which can easily be measured. This thrust is opposed by a quadratic or Rayleigh-type drag force $F_R = \frac{1}{2}\rho C_D A_S v^2$, where ρ is the density of water, C_D the drag coefficient, A_S the submerged cross-sectional area, and v the velocity. (From here on we use “ v ” when referring to boat and “ v_d ” when referring to the ions. Drag for the boat obeys Rayleigh’s law rather than Stokes’ law because it is not dominated by viscosity.) Newton’s second law $Ma = Mdv/dt = F_{\text{net}} = F_{\parallel} - F_R$ then becomes a separable differential equation:

$$\frac{dv}{\alpha - \beta v^2} = dt, \quad (2)$$

where $\alpha \equiv ILB/M$ and $\beta \equiv \frac{1}{2}\rho C_D A_S/M$. If the boat starts from rest at t_0 , integration gives

$$v(t) = \sqrt{\alpha/\beta} \tanh[\sqrt{\alpha\beta}(t - t_0)]. \quad (3)$$

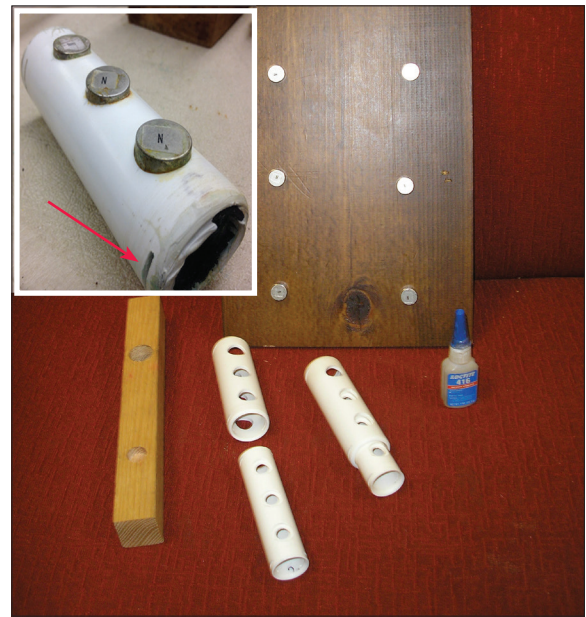


Fig. 5. Magnets and thruster components (below) and after assembly (inset at top). Note “magnet manipulator” (left), magnet polarity labels, and electrode “gill slits” (arrow, inset).

As $t \gg t_0$, the tanh term approaches its asymptotic value of one and the boat reaches *terminal velocity*:

$$v_t = \sqrt{\frac{\alpha}{\beta}} = \sqrt{\frac{2ILB}{\rho C_D A_S}}. \quad (4)$$

For algebra-based classes, Eq. (4) can be obtained more quickly by assuming that equilibrium has already been reached and solving Newton’s *first* law $F_{\text{net}} = 0$ (or $F_{\parallel} = F_R$) directly for v_t . Equation (3), however, turns out to be helpful in what follows, so we retain it here.

Experiment

To test Eqs. (3) and (4), we constructed boats using sturdy 1-L soda bottles (Fig. 4). Each boat was fitted with a thruster fashioned from two nested 5-in lengths of PVC pipe (diameters 1 in and 1 1/4 in), with the gap between the pipes sealed at each end by waterproof caulking (Fig. 5). We drilled six 3/4-in holes at equal intervals in each outer pipe, and inserted six neodymium magnets (3/4 in \times 3/8 in) with a pulling force of 35 lb each. Inserting the magnets was a challenge due to their intense mutual attraction and the fit had to be tight. A “magnet manipulator” (piece of wood with magnet-sized indentations) was helpful, and it was advisable to confirm and mark the polarity of each magnet before insertion. As we learned to our chagrin after completing our tests, finished thrusters should be coated in waterproof urethane to mitigate the effects of corrosion.

The distance between the north and south magnetic poles inside the thruster tube is close to the optimal value identified by Font and Dudley⁵ (i.e., the width of the pole side of each magnet, here 3/4 in). We used a Bell Model 9200 gaussmeter to measure the approximate strength of the vertical component

of the magnetic field (in air) at 63 points inside each thruster tube (Fig. 6). These measurements were tricky. The field is certainly non-uniform, and even changes direction along the tube walls immediately between the magnets (points labeled “D”). In the critical region between the electrodes, however, the direction is constant (points labeled “A,” “B,” and “C”). A straight average of these 49 readings gives $B = 66 \pm 10$ mT (where the uncertainty corresponds to standard error). Alternatively, fitting all the data with a 3D interpolation function and averaging over the volume of the region between the electrodes gives $B = 75 \pm 10$ mT. We adopted an intermediate value with a generous error margin, $B = 70 \pm 15$ mT. This result should not be affected by the presence of seawater; NaCl solutions have a magnetic susceptibility $\chi_m \sim -10^{-5}$ so that their permeability $\mu = (1 + \chi_m)\mu_0$ is essentially the same as that of air.¹⁴

To measure the drag coefficient C_D , we connected each boat to a mass m by a length of lightweight fishing line (linear density 0.05 g/m) that passed over a PASCO low-friction pulley/photogate velocity sensor. This mass was then allowed to fall, producing an approximately constant pulling force on the boat. Replacing $F_{||} = ILB$ with $F_g = mg$ in Eq. (3) gives $v(t)$ in terms of C_D as

$$v(t) = \sqrt{\alpha_m / C_D} \tanh[\sqrt{\beta_m C_D} (t - t_0)], \quad (5)$$

where $\alpha_m \equiv 2mg/\rho A_S$ and $\beta_m \equiv mg\rho A_S/2M^2$. Fitting Eq. (5) to the data then gives a best-fit value of C_D . Our boats had masses $M = 590 \pm 30$ g and total submerged cross-sectional areas $A_S = A_b + A_t + A_m + A_c + A_l = 31 \pm 2$ cm², where $A_b = 17$ cm² (bottle), $A_t = 8$ cm² (thruster tube), $A_m = 2$ cm² (magnets), $A_c = 2$ cm² (clips and electrodes), and $A_l = 2$ cm² (leads). We used test masses m light enough to allow travel times of at least 10 s, but heavy enough that the mass of the line could be neglected. Figure 7 shows the resulting measured velocities as a function of time for three different values of m (points) along with the fits (curves). This procedure was repeated three times, resulting in a best-fit value of $C_D =$

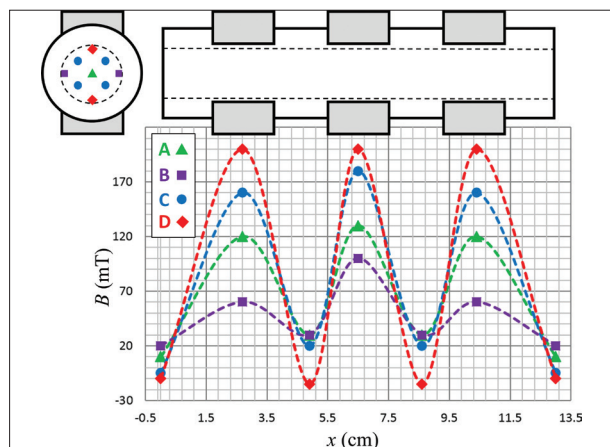


Fig. 6. Front and side views of thruster tubes (top), with magnets (shaded) and locations of B -field measurements (points). The plot (bottom) shows measured values of the vertical component of B connected by trendlines (for visual aid).

1.3 ± 0.2 . This was higher than we had anticipated based on published values for hollow cylinders ($C_D \approx 0.8$)¹⁵ and boat hulls (0.003).¹⁶

To maximize the current, we dissolved 8.00 kg of 99.8% pure NaCl pool salt into deionized H₂O, which then filled a glass aquarium tank (12 in \times 48 in) to a depth of 4.75 in. This resulted in a salt density $\rho_{\text{NaCl}} = 150 \pm 5$ g/L (i.e., a concentration $c = 2.6 \pm 0.1$ mol/L), considerably higher than the standard seawater value of 35 g/L. (It also necessitated a small trade-off with higher fluid density, $\rho = 1114 \pm 5$ kg/m³ at 20 °C.¹⁷) We used an Acumet XL60 salinity meter to measure a resistivity $\rho_e = 0.055 \pm 0.005$ Ω m, just over the accepted saturation value.¹²

The electric field was provided by six standard 9V batteries inside each bottle, connected by leads and alligator clips to the electrodes inside the thruster tubes (Fig. 4). Thanks to their metal casings, the battery packs clamped firmly to the magnets, effectively fastening the bottles to the thruster tubes. The electrodes consisted of strips of heavy copper or aluminum foil, cut to a width $w = 1.2 \pm 0.1$ cm. (Performance did not differ significantly between the two metals.) The distance between the electrode “gill slits” was $l = 11.4 \pm 0.2$ cm, so that the electrode area $A_e = lw = 14 \pm 1$ cm². The electrodes were separated by a mean distance slightly less than the inner diameter of the thruster tube, $L = 2.0 \pm 0.1$ cm.

The arrangement of the batteries makes for some illuminating concept questions. Given that $v_t \propto \sqrt{I}$ in Eq. (4), a student who thinks of batteries as sources of constant current will try to maximize speed by connecting all six batteries in *parallel*. A more sophisticated student who thinks of batteries in terms of constant voltage may use Ohm’s law, $I = V/R$, and attempt to maximize speed instead by connecting all six batteries in *series*, reasoning (correctly) that this should give the greatest V . Both are wrong, because they have neglected the internal resistance r of the batteries, which becomes very significant in what is essentially a short circuit.

To see this, we use Kirchhoff’s loop rule to obtain $I = n\varepsilon/(R$

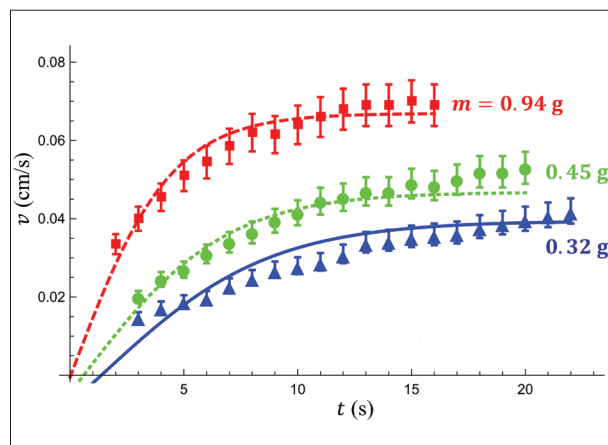


Fig. 7. Measured boat speeds as a function of time for three different pulling masses m (data points) with predictions from Eq. (5) assuming a best-fit drag coefficient $C_D = 1.3$ (lines).

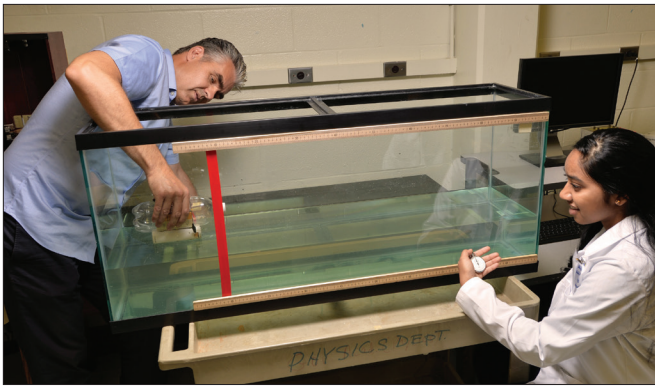


Fig. 8. Two of the authors conducting a timed trial.

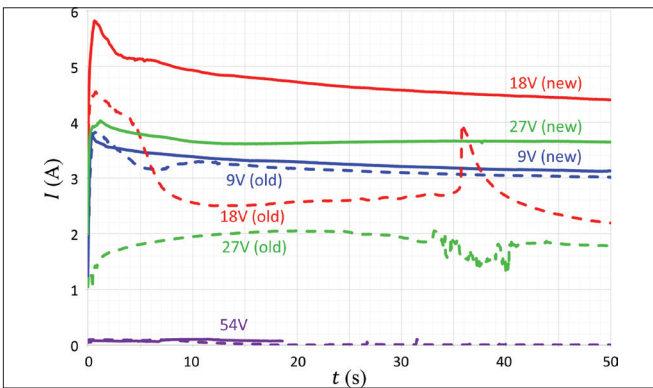


Fig. 9. Measured current for various battery configurations (9 V, 18 V, 27 V, and 54 V; see text for discussion) after initial timed run (solid) and subsequent trials (dashed).

+ nr), where n is the number of batteries in series, each with a nominal emf $\varepsilon = 9.0 \pm 0.3$ V. The resistance of the saltwater between the electrodes is very low, $R = \rho_e L/A_e = 0.8 \pm 0.1 \Omega$. To measure the current as realistically as possible, we interspersed our timed runs with “current runs” where the boats were placed in the water while connected to a PASCO current sensor. (Naturally this was not possible during the timed runs themselves.) We conducted 30 trials using three different battery arrangements (Fig. 8). The most reliable results were obtained in the parallel case ($n = 1$, “9 V”). Currents were initially higher when arranged in a 2×3 ($n = 2$, “18 V”) or 3×2 configuration ($n = 3$, “27 V”), but they dropped rapidly during successive runs, presumably due to increasing internal resistance, as each individual battery in those cases needed to supply a larger fraction of the total measured current.

Results are plotted in Fig. 9 and summarized in Table I, along with the inferred thrust force $F_{||}$ from Eq. (1) and predicted terminal velocity from Eq. (4). We also tried a 1×6 series combination ($n = 6$, “54 V”), but the batteries in this case were depleted before the boat crossed the tank. (Batteries in the higher-voltage configurations became noticeably hot with use, and also led to some uncomfortable shocks, particularly with the high salt concentrations used here.) To minimize systematic effects, we conducted our trials in sets, cycling through each battery pack (i.e., 9 V followed by 18 V, then 27 V, etc.). The numbers above imply that internal resistances

Table I. Average measured current I , with corresponding Lorentz thrust force $F_{||}$ and predicted terminal velocity v_t .

	I (A)	$F_{ }$ (mN)	v_t (cm/s)
9 V	3.3 ± 0.5	4.6 ± 1.2	4.5 ± 0.7
18 V	3.5 ± 1.5	4.9 ± 2.4	4.7 ± 1.2
27 V	2.5 ± 1.5	3.5 ± 2.2	3.9 ± 1.3

Table II. Measured mean speed \bar{v} and terminal velocity v_t based on the fits in Fig. 10, with corresponding drag force F_R .

	\bar{v} (cm/s)	v_t (cm/s)	F_R (mN)
9 V	3.2 ± 0.1	4.0 ± 0.9	3.6 ± 1.7
18 V	2.7 ± 0.2	3.4 ± 0.9	2.6 ± 1.4
27 V	2.7 ± 0.3	3.0 ± 0.7	2.0 ± 1.0

averaged $r = 1.9 \pm 0.4 \Omega$, $2.2 \pm 1.0 \Omega$ and $3.3 \pm 2.1 \Omega$ for the 9 V, 18 V, and 27 V configurations, respectively. The fact that best results are obtained near $R \sim r$ may be seen as an example of the general principle of impedance matching.

Results

Average measured boat speeds \bar{v} were about one-third slower than the predicted terminal speeds v_t in Table I (see Table II, where the uncertainties are statistical standard errors). Our error budget was dominated by uncertainties in current I , magnetic field B , and drag coefficient C_D (in that order), and some of the discrepancy between v_t and \bar{v} may be due to systematic error in one or more of these quantities. Another factor, however, came to light when we plotted speed \bar{v} versus travel distance d (Fig. 10). Different distances arose in practice because the boats did not necessarily travel in a straight line, but occasionally turned toward one side of the tank. We ended each run when a wall was struck. (This turning effect was likely due primarily to small random misalignments between the thruster tube and the body of the boat.) We discussed ways to mitigate this behavior, but in retrospect the range of travel distances proved to be advantageous in analyzing our results. Figure 10 reveals that the boats were accelerating during much of their $\sim 30 \pm 15$ s trial times, so that they only reached terminal velocity near the end of their runs. The same behavior is evident in Fig. 7, and indeed the gravitational driving forces there ($3.1 \text{ mN} \leq mg \leq 9.2 \text{ mN}$) are comparable to the magnetic thrust forces in Table I.

To extract the value of v_t from this range of values of \bar{v} for different distances d , we note from Eq. (3) that velocity at time t can be expressed in terms of v_t by $v(t) = v_t \tanh(t/\tau)$, where τ is a constant. Integration gives the travel distance $d(t) = \int v(t) dt = v_t \tau \ln[\cosh(t/\tau)]$. Trigonometric identities then imply that

$$v(d) = v_t \sqrt{1 - \exp(-2d/v_t \tau)}. \quad (6)$$

Fitting Eq. (6) to the data, we obtain the curves shown in Fig. 10, with corresponding best-fit values of v_t listed in Table II

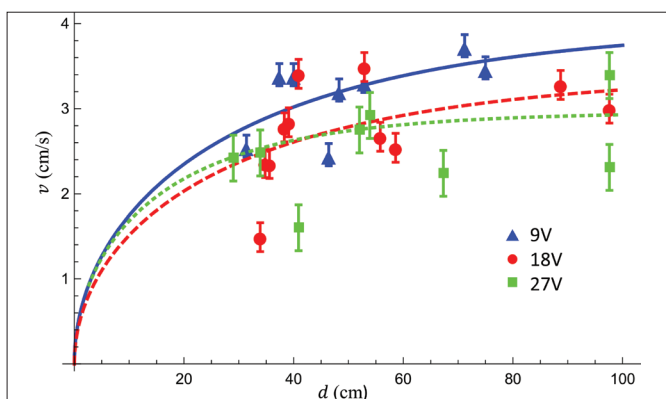


Fig. 10. Measured boat speeds as a function of travel distance (points) with fits to Eq. (6) (curves), allowing us to extrapolate and obtain the terminal velocity in each configuration.

along with drag forces $F_R = \frac{1}{2}\rho C_D A_S v_t^2$. [Uncertainties here are given by the standard error of the fit. This fitting procedure works less well when speed is plotted against time instead of distance, because of the sensitivity of $\tanh(t/\tau)$ to the value of τ .] The terminal speeds v_t in Table II are still slightly smaller than those predicted in Table I, but the two sets of numbers are now consistent within their margins of error.

There is rich scope here for deeper investigation at a level that is well suited to student research. The fact that the boats take some time to reach terminal velocity raises the question whether drag is really of the quadratic (Rayleigh) type, as assumed in Eq. (2). This assumption can be checked using the Reynolds number $Re = \rho v D / \eta$, where D is a characteristic size and dynamic viscosity $\eta = 1.47 \times 10^{-3} \text{ kg}\cdot\text{s}^{-1}\cdot\text{m}^{-1}$ for saltwater at the concentration used here.¹⁷ The Stokes limit corresponds to $Re \ll 1$ (viscous or “creeping flow”) while Rayleigh’s law is derived under the condition $Re \gg 1$ (when the behavior of the fluid is dominated by its own momentum).¹⁸ The values of “critical” Reynolds numbers separating one type of behavior from another depend on the medium and shape of the body, but the onset of turbulence is certainly a sign that one is in the Rayleigh regime. Turbulence is found in flow over flat surfaces when $Re \gtrsim 600$,¹⁸ and in flow through circular pipes when $Re \gtrsim 2000$ (where D is the inner pipe diameter).¹⁹

For our boats, $v \approx 3.0 \text{ cm/s}$ and $D \approx 2.5 \text{ cm}$, so $Re \approx 600$, putting us near the intermediate regime where *neither* limit is valid. The surprisingly high values of C_D we measured may thus reflect unexpectedly strong viscosity. We could increase Re by reducing salt concentration (and hence η), but this would also reduce the current. Widening the boat (to increase D) would weaken the magnetic field.⁵ From an experimental point of view, the most effective way to reduce viscous drag is probably to improve the aerodynamics of our boats and thruster tubes (perhaps with the help of a lighter power supply and/or catamaran-style design, as on the *Yamato-1*). Alternatively, from the theoretical point of view, one might try modeling drag force with a *combination* of Stokes and Rayleigh terms, $F_d = c_S v + c_R v^2$.

One might ask what fraction of the ions inside the thruster

actually participate in the current that drives the boat. We attempt to answer this question in an online appendix²⁰ concluding that *nearly all the ions present are helping to push the boat*. This in turn suggests that stray currents (i.e., those not passing through the magnetic field) are not one of the major limiting factors in our design.

Discussion

Students respond creatively when challenged to think of ways to increase the speed of the boat. Given that thrust is proportional to the transverse drift velocity v_d of the ions, it occurred to one of the authors that the “turning effect” exhibited during many of our trials might be due partly to the fact that Na^+ and Cl^- drift at *different speeds*. (The lighter Na^+ ions are slowed down more by interactions with water molecules.) As they migrate in opposite directions, the two ion populations gradually²⁰ become segregated, so that different thrust might be produced by the ions on either side of the boat.

Specifically, the values and expressions derived in the online appendix imply that $v_{d,\text{Na}} = u_{\text{Na}} V/L = 4 \mu\text{m/s}$ for Na^+ and $v_{d,\text{Cl}} = u_{\text{Cl}} V/L = 6 \mu\text{m/s}$ for Cl^- , with a mean $\bar{v}_d = 5 \mu\text{m/s}$ (all numbers here assume the 9 V case). The thrust produced by each ion population is $F_{\parallel} = (N/2)eBv_d = 2 \text{ mN}$ for Na^+ and 3 mN for Cl^- , so the difference $\Delta F_{\parallel} = 1 \text{ mN}$. During each time interval dt , their mean segregation distance increases by $dx = (v_{d,\text{Na}} + v_{d,\text{Cl}})dt = 2 \bar{v}_d dt$. This changes the torque on the boat by $d\tau = \Delta F_{\parallel} dx \equiv I_M d\alpha$, producing a corresponding change in angular acceleration $d\alpha$ where $I_M = (M/12)(L^2 + W^2)$ is the moment of inertia for a rectangular mass M of length L and width W . With $M = 590 \text{ g}$, $L = 13 \text{ cm}$, and $W = 4 \text{ cm}$, we find $d\alpha = \dot{\alpha} dt$, where $\dot{\alpha} \equiv 2\Delta F_{\parallel} \bar{v}_d / I_M = 1 \times 10^{-5} \text{ rad/s}^3$. Integration then gives the angular acceleration $\alpha = \int d\alpha = \dot{\alpha} t$, angular velocity $\omega = \int \dot{\alpha} dt = \frac{1}{2} \dot{\alpha} t^2$, and turning angle $\theta = \int \omega dt = (1/6) \dot{\alpha} t^3 \lesssim 10^\circ$ for $t \lesssim 45 \text{ s}$. A turning effect this small would likely be masked by random uncertainties. To put it another way, at an average speed $\bar{v} \approx 4 \text{ cm/s}$ the associated radius of curvature $R = \bar{v} t / \theta \gtrsim 10 \text{ m}$, much larger than the length of our tank.

To look for such an effect nonetheless, we connected two boats together with struts and ran two sets of 12 tests each: one with the thruster tubes aligned the same way (for maximum turning effect), and the other with the thruster tubes *anti-aligned* (i.e., one tube upside down, thus nulling out the effect since the directions of both the magnetic and electric fields are reversed). To minimize systematic error, we also reversed the direction of travel between each trial. Our results provided weak evidence, at best, for a systematic turning effect. When the thrusters were aligned, the boats turned both ways almost equally often (7 “right,” 4 “wrong,” and 1 “both”) with a mean turning radius $|R| = 1.1 \text{ m}$. When anti-aligned (control group) the direction was slightly more “random” as expected (6 “right,” 5 “wrong,” 1 “both”), but the mean radius decreased, $|R| = 0.5 \text{ m}$. Improved tests for this effect will require better control of random effects such as wave motion, initial orientation, and misalignment between the thruster

tube and boat body. The experiments must of course be carried out far from ferromagnetic materials. (It is amusing to note that a similar “turning effect” was noticed in early tests of small-scale prototypes for the *Yamato-1* and ultimately traced to the influence of Earth’s magnetic field.⁸)

Another suggestion involved the “Venturi effect” employed in jet engines and automotive carburetors, whereby the thruster tube narrows from front to back so that seawater is forced to speed up as it passes through. But will this also speed up the boat? We will not spoil the story here, but note that it is easy to test the matter by fitting the thruster tube with a conical nozzle like those sold with handheld vacuum cleaner kits (we obtained ours at the same hardware chain where we bought the pipes). Useful background information is found in Ref. 7.

Conclusion

MHD drive works! Within experimental uncertainties, our results confirm that measured speeds agree with theoretical predictions, whether expressed in terms of current or mobility. Whether this form of propulsion is *silent*, though, is another question. Copious bubbles were produced by chemical reactions near the positive electrode (Fig. 4). In a scaled-up model these bubbles would produce considerable noise,⁹ defeating much of the system’s original purpose. Moreover, acoustic noise is not the only problem. An MHD-driven submarine could be tracked by its trail of chlorine ions and metal chlorides,⁵ or by the intense magnetic field itself. These factors, along with the challenge posed by navigating in freshwater ports and waterways, have been cited as the main reasons for the lack of sustained military interest in pursuing the promise of MHD propulsion.⁸

A second major class of problems involves the electrodes, which reacted so rapidly with the chlorine ions that they became severely corroded, increasing the resistance R and decreasing I . (Helpful discussion of these chemical reactions is found in Ref. 7.) Whether made of copper or aluminum, they became so thin and brittle that they had to be replaced every few runs. As noted by Font and Dudley,⁵ any scaled-up MHD boat would likewise need to replace its electrodes on a regular basis, or use more advanced materials. (The 3.4-m long electrodes on the *Yamato-1* used titanium alloy as a base metal, with aluminum plating on the cathode and DSA or “dimensionally stable anode” ruthenium oxide coating on the anode.⁴)

Finally, the biggest limiting factor in our boats turned out to be the power supply. Were we to repeat our experiments, we would begin by looking for lighter and more powerful batteries. The same limitation applies even more strongly on larger scales. A full-size vessel would need an onboard generator, not only to supply the electric field but also in the coils generating the magnetic field. (Permanent magnets, of course, would not suffice on these scales; and in fact, the coils would likely need to be superconducting to attain the required field strengths, thus adding a third element to the

onboard power requirements.) The *Yamato-1* attained $I \sim 2000$ A and $B \sim 4$ T with a propulsion system that filled most of the ship (leaving room for only 10 people in a cramped cockpit) and accounted for 70% of the total vessel weight,⁸ and even then the largest components (for pre-cooling the superconducting coils) had to be housed onshore.⁴ Font and Dudley have estimated that to power a *Trident*-class submarine the same way would require either $B \sim 435$ T or $I \sim 540,000$ A.⁵ Developments in science and technology may someday allow fields and currents this strong, but their generation would almost certainly require many moving parts. The world might tremble at the weight of such a craft, but not at its silence.

Despite its limitations, however, MHD drive provides a simple and beautiful demonstration of electromagnetism in action, with applications that go well beyond maritime propulsion and extend all the way to space. NASA’s *Dawn* mission to the asteroids Vesta and Ceres uses an ion drive based on the same principle (except, of course, that the density of ions present in interplanetary space is much too low to provide an effective thrust, so the spacecraft carries its own onboard supply).²¹ For students, the MHD boat functions perhaps most effectively as a reminder of the importance of Newton’s third law, the use of the right-hand rule, and, above all, the physical reality of the electromagnetic field. The “equal and opposite force” of the seawater ions, after all, acts on this *field*—yet it pushes the boat forward just as surely as if they were connected by springs. Students who experience this reality with their own eyes are thereby ushered to the threshold of modern physics.

Acknowledgments

We thank Mark Edmonston, Jeff Klupt, Bob Kuta, and the late Mark Scarinzi for their considerable help in building our boats, and the anonymous referees for invaluable advice on improving the manuscript. This research was supported in part by a grant from the Faculty Development and Research Council of Towson University.

References

1. In Clancy’s novel, *Red October*’s propulsion system was not magnetohydrodynamic but based on a more conventional (but also unusually quiet) “pump-jet” system employed in the massive *Typhoon*-class Soviet submarines of the 1980s. Nevertheless, there was intense real-world suspicion during this period that the Soviets were developing MHD-driven attack submarines. As late as 1990, military analysts were convinced that strange “pods” mounted on the tails of new Soviet *Victor III*-class submarines were MHD thrusters [“Evidence grows the ‘pod’ is a superconductive drive,” *Navy News and Undersea Technol.* 7 (11), 1–2 (March 19, 1990)]. Attempts to photograph these pods caused a collision with a U.S. Navy ship, the *U.S.S. Drum*, in 1981 [W. C. Reed, *Red November: Inside the Secret U.S.-Soviet Submarine War* (William Morrow, 2010)].
2. S. Way, “Electromagnetic propulsion for cargo submarines,” *J. Hydraulics* 2, 49–57 (1968).

3. A. Iwata, Y. Saji, and S. Sato, "Construction of Model Ship ST-500 with Superconducting Electromagnetic Thrust System," in *Proceedings of the 8th International Cryogenic Engineering Conference, ICEC 8*, edited by C. Rizzuto (IPC Science and Technology, 1980), pp. 775–784.
4. S. Takezawa et al., "Operation of the thruster for superconducting electromagnetohydrodynamic propulsion ship YAMA-TO-1," *Bull. Marine Eng. Soc. Japan* **23**, 46–55 (1995); available online at <http://www.jime.jp/e/publication/bulletin/english/pdf/mv23n011995p46.pdf>, accessed April 25, 2017.
5. G. I. Font and S. C. Dudley, "Magnetohydrodynamic propulsion for the classroom," *Phys. Teach.* **42**, 410–417 (Oct. 2004); erratum **42**, 517 (Dec. 2004).
6. O. M. Phillips, "The prospects for magneto-hydrodynamic ship propulsion," *J. Ship Res.* 43–61 (March 1962).
7. J. B. Gilbert and T. F. Lin, "Studies of MHD propulsion for underwater vehicles and seawater conductivity enhancement," Pennsylvania State University Applied Research Laboratory Report AD-A231 623, 1–114 (Feb. 1991); online at <http://www.dtic.mil/dtic/tr/fulltext/u2/a231623.pdf>, accessed April 25, 2017.
8. D. Normile, "Superconductivity goes to sea," *Pop. Sci.* **241**, 80–85 (Nov. 1992).
9. K. E. Tempelmeyer, "Electrolysis bubble noise in small-scale tests of a seawater MHD thruster," preprint DTRC-90/30 (David Taylor Research Center, Bethesda, MD, Sept. 1990); online at <http://www.dtic.mil/dtic/tr/fulltext/u2/a227548.pdf>, accessed April 25, 2017.
10. W. H. Van den Berg and K. A. Miller, "Moving water with no moving parts," *Phys. Teach.* **35**, 531 (Dec. 1997).
11. J. D. Wilson, A. J. Buffa and B. Lou, *College Physics* (Addison-Wesley, 2002), p. 667.
12. H. Semat and R. Katz, *Physics* (Rinehart, 1958), p. 526; author edition available online at <http://digitalcommons.unl.edu/physickatz/188/>. Neutron diffraction experiments reveal that these hydration shells contain, on average, five H₂O molecules for Na⁺ and six for Cl[−], with "inner" and "outer radii" of about 200 pm and 300 pm respectively, regardless of concentration; see R. Mancinelli et al., "Hydration of sodium, potassium, and chloride ions in solution and the concept of structure maker/breaker," *J. Phys. Chem. B* **111**, 13570–13577 (2007).
13. P. W. Atkins, *Physical Chemistry*, 4th ed. (W. H. Freeman, 1990), p. 755.
14. H. Seo, "Measurement of the magnetic susceptibility of liquids," University of Minnesota preprint (Spring 2013); available online at <https://sites.google.com/a/umn.edu/mxp/home/2013---spring/s13magneticsusceptibilityliquids>, accessed April 25, 2017.
15. B. Franzluebbers, "Drag coefficients of inclined hollow cylinders: RANS versus LES," Worcester Polytechnic Institute preprint (April 2013); available online at <https://web.wpi.edu/Pubs/E-project/Available/E-project-042313-161611/unrestricted/MQP.pdf>, accessed April 25, 2017.
16. C.-W. Lin, S. Percival, and E. H. Gotimer, "Viscous drag calculations for ship hull geometry," preprint, Naval Surface Warfare Center, Carderock Division, Bethesda, MD, Ship Hydrodynamics Department (1995); available online at <http://www.dtic.mil/get-tr-doc/pdf?AD=ADA323498>, accessed April 25, 2017.
17. M. H. Sharqawy, J. H. Lienhard, and S. M. Zubair, "The thermophysical properties of seawater: A review of existing correlations and data," *Desalination and Water Treatment* **16**, 354–380 (2010); online at <http://web.mit.edu/seawater/>, accessed April 25, 2017.
18. G. K. Batchelor, *An Introduction to Fluid Dynamics* (Cambridge University Press, 2000), pp. 233, 335.
19. V. Thomsen, "Estimating Reynolds number in the kitchen sink," *Phys. Teach.* **31**, 410 (Oct. 1993).
20. See the appendix under the "Supplemental" tab at *TPT Online*, <http://dx.doi.org/10.1119/1.5008337>.
21. Z. J. Brophy, "The Dawn ion propulsion system," *Space Sci. Rev.* **163**, 251–261 (2011).

James Overduin is an associate professor in the Department of Physics, Astronomy and Geosciences at Towson University, where he has supervised more than 25 undergraduate research students in projects ranging from experimental demonstrations for introductory electromagnetism to advanced topics in astrophysics, cosmology, and gravitation.
<http://wp.towson.edu/joverdui/>; joverduin@towson.edu

Viktor Polyak was a sophomore when he worked on this project in the fall of 2014. He developed alternative MHD thruster designs using a 3-D printer and won an award for "Best Student Presentation" at a regional meeting of the AAPT (Chesapeake Section) at Loyola University. He plans to become a physics teacher.
vikpolyak@gmail.com

Anjalee Rutah was a high school research intern from the Bryn Mawr School in Baltimore when she worked on this project during the summer of 2015, measuring currents, magnetic field strengths, and travel times for our final set of boats. She is now a freshman at Colby College.
anjalee.rutah@colby.edu

Thomas Sebastian was a junior when he began this project with Dr. Overduin in the fall of 2013. He developed and tested our first prototypes, and presented preliminary results at a regional meeting of the AAPT (Chesapeake Section) at the University of College Park in the spring of 2014. He is now a reliability engineer with the U.S. Naval Air Systems Command (NAVAIR).
tjsebastian93@gmail.com

Jim Selway is a resident Master Teacher in the Department of Physics, Astronomy and Geosciences at Towson University. With more than 40 years of high school physics teaching under his belt, he is the department's secret weapon, helping the faculty design and implement new ways to reach their students through lab exercises and teaching demonstrations.
jselway@towson.edu

Dan Zile worked on this project as a junior and senior from 2014–15, culminating in a capstone research course during the summer of 2015. He helped in the design and construction of our final set of boats, collected nearly all the data, and presented our final results at the 2016 APS March meeting in Baltimore. He is now a first-year graduate student in physics at Carnegie-Mellon University.